



Drp1-mediated mitochondrial fission contributes to mitophagy in paraquat-induced neuronal cell damage[☆]

Nengzhou Chen^{a,1}, Zhenkun Guo^{b,c,1}, Zhousong Luo^a, Fuli Zheng^{a,b,c}, Wenya Shao^a, Guangxia Yu^{a,b,c}, Ping Cai^e, Siying Wu^{b,c,d}, Huangyuan Li^{a,b,c,*}

^a Department of Preventive Medicine, School of Public Health, Fujian Medical University, Fuzhou, 350122, China

^b The Key Laboratory of Environment and Health, School of Public Health, Fujian Medical University, Fuzhou, 350122, China

^c Fujian Provincial Key Laboratory of Environment Factors and Cancer, School of Public Health, Fujian Medical University, Fuzhou, 350122, China

^d Department of Epidemiology and Health Statistics, School of Public Health, Fujian Medical University, Fuzhou, 350122, China

^e Department of Health Inspection and Quarantine, School of Public Health, Fujian Medical University, Fuzhou, 350122, China

ARTICLE INFO

Article history:

Received 13 July 2020

Received in revised form

20 December 2020

Accepted 29 December 2020

Available online 31 December 2020

Keywords:

Mitophagy

Mitochondrial fission

ROS

DRP1

Paraquat

ABSTRACT

Paraquat (PQ) is one of the most widely used herbicides in the world due to its excellent weed control effects. Accumulating evidence has revealed that long-term exposure to PQ can significantly increase the risk of Parkinson's disease (PD). However, the underlying molecular mechanisms are yet to be fully understood. Hence, we investigated the potential role of reactive oxygen species (ROS) and dynamin-related protein 1 (DRP1) in PQ-induced mitophagy, aiming to elaborate on possible molecular mechanisms involved in PQ-triggered neurotoxicity. Our results showed that ROS were increased, mitochondrial membrane potential was decreased at 100, 200, and 300 μ M PQ concentrations, and autophagy pathways were activated at a concentration of 100 μ M in neuronal cells. In addition, excessive mitophagy was observed in neurons exposed to 300 μ M PQ for 24 h. Then, ROS-mediated mitochondrial fission was found to contribute to PQ-induced excessive mitophagy. Moreover, all aforementioned changes were significantly ameliorated by mdivi-1. Thus, our findings provide a novel neurotoxic mechanism and reveal the DRP1-mitochondrial fission pathway as a potential target for treatments of PQ-induced excessive mitophagy, serving as an alternative target for the prevention and treatment of Parkinson's disease. Because harmful substances are transmitted and enriched in the food chain, the toxic effect of environmental paraquat is nonnegligible, and more investigations are needed.

© 2021 Elsevier Ltd. All rights reserved.

Abbreviations: ATG12, Ubiquitin-like protein ATG12; Ambra1, Activating molecule in BECN1-regulated autophagy protein 1; Bfa1, Bafilomycin A1; COX IV, Cytochrome c oxidase subunit 4 isoform 1 mitochondrial; CQ, Chloroquine; DRP1, Dynamin-Related Protein 1; FIS1, Mitochondrial fission 1 protein; Hsp60, 60 kDa heat shock protein mitochondrial; ROS, Reactive oxygen species; SQSTM1/p62, Sequestosome-1; OPA1, Dynamin-like 120 kDa protein mitochondrial; PD, Parkinson's disease; PINK1, Serine/threonine-protein kinase PINK1 mitochondrial; PQ, Paraquat; Parkin, E3 ubiquitin-protein ligase parkin; TOMM20, Mitochondrial import receptor subunit TOM20 homolog; LC3B, Microtubule-associated proteins 1A/1B light chain 3B; MMP, Mitochondrial membrane potential; Mito, mitotracker; Lyso, lysotracker; mTOR, Serine/threonine-protein kinase mTOR; MFN2, Mitofusin-2; MAP2, Microtubule-associated protein 2; NAC, N-Acetylcysteine; h, hours; NBR1, Next to BRCA1 gene 1 protein; VDAC1, Voltage-dependent anion-selective channel protein 1.

[☆] This paper has been recommended for acceptance by Sarah Harmon.

* Corresponding author. Department of Preventive Medicine, School of Public Health, Fujian Medical University, Fuzhou, 350122, China.

E-mail address: lhy@fjmu.edu.cn (H. Li).

¹ Nengzhou Chen and Zhenkun Guo contributed equally to this work.

Authors' contributions

Nengzhou Chen: conducted the main experiments and analyzed results, wrote the original draft. Zhen-kun Guo: conducted the main experiments and analyzed results. Zhou-song Luo: participated to some of the experiments. Fu-li Zheng: contributed to facilitate the quality of the article. Wen-ya Shao: contributed to facilitate the quality of the article. Guang-xia Yu: contributed to facilitate the quality of the article. Ping Cai: contributed to facilitate the quality of the article. Si-ying Wu: designed and monitored the progress of the research. Huang-yuan Li: conceptualized the hypotheses, and reviewed and facilitated the scientific quality of manuscript.

1. Introduction

Paraquat (1,1'-dimethyl-4,4'-bipyridium dichloride, PQ) is one of

the most widely used herbicides in the world. In the United States in 2012, the US Environmental Protection Agency (EPA) reported that 2–6 million pounds of PQ were used for agricultural purposes (Cao et al., 2019a). The abuse of PQ might cause potential damage to humans and the surrounding environment. The ecological risks of PQ were foreseeable because it was closely linked to erosive sediments that might be transported to surface water (Amondham et al., 2006; Rashidipour et al., 2019). It causes toxic and teratogenic effects in amphibians and toxic effects in honeybees, fish, and other aquatic species (Sartori and Vidrio, 2018; Xu et al., 2018). Most strikingly, both epidemiologic and laboratory evidence indicate that long-term sublethal exposure to PQ may cause neurotoxicity in humans, especially Parkinson's disease (PD) (Chinta et al., 2018; Mostafalou and Abdollahi, 2017; Wang et al., 2017). PD is a progressive neurodegenerative disease characterized by motor symptoms, such as bradykinesia, tremor, gait, and postural abnormalities. Approximately 1–2% of the world's population over 65 years old suffers from PD (Pringsheim et al., 2014). One study reported that the incidence of PD was related to the cumulative days of the subject using pesticides, in which the odds ratio was 2.3, and the 95% confidence interval was 1.2–4.5 (Kamel et al., 2007). Nevertheless, there is currently no objective diagnosis or effective treatment (Friedman, 2019; Kalia and Lang, 2015; Kühlenbäumer and Berg, 2019).

Several studies have been conducted to pinpoint possible mechanisms between PQ and PD, yet to our knowledge, the vast majority of related studies have indicated that the main culprit might be oxidative stress caused by PQ (Baltazar et al., 2014; Li et al., 2019; Marras et al., 2019; Zheng et al., 2020). Although the pathogenic mechanisms of PD are not completely clear, several lines of evidence suggest that mitochondrial dysfunction could be central to the disease (Bose and Beal, 2016, 2019; Rani and Mondal, 2020). Defective mitochondria, if left unattended, could compromise the health of the entire mitochondrial network (Bingol et al., 2014). Noticeably, mitophagy is a specialized autophagy pathway mediated by lysosomes to eliminate damaged mitochondria and is important for mitochondrial quality control (Chen et al., 2017; Soutar et al., 2019). PINK1 and Parkin are key components of the mitochondrial quality control system (Bonello et al., 2019; Niu et al., 2020). PINK1 phosphorylates ubiquitin at S65 and activates Parkin to recruit damaged mitochondria (Nguyen et al., 2016). In the last decade, the key role of autophagy in neuronal homeostasis has been established, and autophagy destruction has been shown to cause neurodegeneration (Heckmann et al., 2019; Sathiyaseelan et al., 2019; Stavoe and Holzbaur, 2019).

Various studies have indicated that alterations in mitochondrial dynamics might be one of the underlying pathological mechanisms of PD (Ge et al., 2020; Ordonez et al., 2018). Toxin-induced loss of dopaminergic neurons (MPP⁺: 10⁻⁴ mol/L, 4 h; MPTP: 20 mg/kg, i. p., 5 days; MPP⁺: 0–4 mM, 24 h) has linked neurotoxicity to excessive mitochondrial fragmentation mediated by DRP1, suggesting that dysfunction of mitochondrial fission might be critical for the pathogenesis of PD (Chuang et al., 2016; Filichia et al., 2016; Zhang et al., 2019). It was believed that mitochondrial fission occurred first, and then the formation of autophagosomes occurred subsequently, with mitochondria as a process of phagocytosis (Yamashita et al., 2016). However, the association between these alterations and mitophagy has received limited investigation in the nervous system. The underlying mechanisms by which PQ affects neuronal mitophagy are not fully understood.

Based on these premises, 100, 200, and 300 μM PQ concentrations were used in this study to investigate mitophagy-related neuron pathological alterations and to explore the role of Drp1-mediated mitochondrial fission in mitophagy and ROS activation

in neurons.

2. Materials and methods

2.1. Reagents

The following reagents were purchased: LysoTracker Red DND-99 (ThermoFisher, L7528); Mitotracker™ Deep Red (ThermoFisher, M22426); Paraquat dichloride hydrate (Sigma-Aldrich, 36,541); Protease inhibitor cocktail (MCE, HY-K0010); phosphatase inhibitor cocktail I (MCE, HY-K0021); chloroquine (MCE, HY-17589); bafilomycin (MCE, HY-100558); and acetylcysteine (MCE, HY-B0215).

Primary antibodies used for western blotting included Beclin1 (Abcam, ab207612), GAPDH (Abcam, ab181602), SQSTM1/p62 (Abcam, ab109012), LC3B (Abcam, ab51520), Ambra1 (CST, 24,907), mTOR (CST, 2972), p-mTOR Ser 2448 (CST, 2971), NBR1 (CST, 9891), ATG12 (CST, 4180), DNM1L/DRP1 (Abcam, ab184247), FIS1 (Abcam, ab71498), MFN2 (Abcam, ab124773), PINK1 (Abcam, ab23707), TOMM20 (Abcam, ab186735), Hsp60 (Abcam, ab59457), MAP2 (Abcam, ab32454), OPA1 (Abcam, ab157457), PARKIN (Abcam, ab77924), COX IV (CST, 4844), and VDAC1 (Abcam, ab15895). Secondary antibodies were purchased from Sigma-Aldrich (anti-rabbit: AP132P; anti-mouse: AP124P) for western blotting and from Abcam for immunocytochemistry (Abcam, ab175475, ab150063, and ab150109).

2.2. Cell culture

Neuro-2A (N2a) is a mouse neural crest-derived cell line that has been extensively used to study neuronal differentiation, axonal growth, and signaling pathways (Cai et al., 2019; Tremblay et al., 2010). N2a cells were purchased from the cell bank of the Chinese Academy of Sciences (Shanghai, China). N2a cells were cultured in DMEM supplemented with 10% fetal calf serum, 100 units/ml of penicillin, and 100 μg/ml of streptomycin. Cells were incubated at 37 °C in a humidified atmosphere of 5% CO₂ and 95% air. Cell cultures were maintained under logarithmic growth conditions.

2.3. Primary neuronal cultures

We cultured and purified primary neurons from the cerebral cortex of C57BL/6 mice in accordance with previous descriptions with slight modifications (Kang et al., 2020). Postnatal P1–2 mouse pups were used for primary neuron isolation. The cerebral cortex was dissected and placed in a digestion solution containing 2 units/ml papain (Worthington, LS003119), 20 mM EBSS (Thermo Fisher Scientific, 15630080), DNase (50 units/ml, Worthington, LS002139), and EDTA (1 mM) for 20 min. The tissue was dissociated using a 1 ml pipette by gentle trituration. The dissociated tissue was centrifuged at 200 g for 5 min, and the cell pellet was resuspended in neurobasal medium (Thermo Fisher Scientific, 21103049) containing 2% B27 supplement (Thermo Fisher Scientific, 17504044). The obtained neuronal cells were kept in a humidified 5% CO₂ atmosphere at 37 °C. The purity identification showed that primary neurons were greater than 90% (Fig. S5). The animal protocol was approved by the Animal Care and Use Committee of Fujian Medical University.

2.4. PQ treatment

Cells were treated with 100, 200, or 300 μM PQ based on our previous studies (Wang et al., 2018a,b; Yang et al., 2020). The concentration of PQ was chosen for the following reasons. One

study showed that mitophagy increased significantly when SH-SY5Y cells were treated with 0.5 mM paraquat for 24 h (Ramirez-Moreno et al., 2019). Another study showed that fibroblasts were treated with 1 mM and 2 mM PQ for 2 h, and LC3-II protein increased significantly (Wang and Miller, 2012). In addition, a study showed that the mitophagy of A549 cells was significantly increased after treatment with 200 μ M PQ for 24 h (Liu et al., 2020). In order to determine the time point when paraquat induced mitophagy in N2a cells, 100, 200, and 300 μ M PQ for 3, 6, 12, and 24 h was designed for the experiment.

2.5. Measurement of ROS production

N2a cell lines (1.5×10^4) were treated with PQ (0, 100, 200, or 300 μ M) or pretreated with 10 mM NAC for 2 h (Li et al., 2007) followed by 3 h of 200 μ M PQ treatment. DCFH-DA (1 μ M) was added to the cultured cells, followed by incubation at 37 °C for 15 min. The cells were harvested and washed 3 times with ice-cold PBS. Cells were placed on ice for 15 min to stabilize the fluorescence. Then, the fluorescence intensity (FL-1 channel) was detected by flow cytometry (FACS-Calibur, BD). The percentage of cells with elevated ROS in 30,000 cells was counted by flow cytometry. The experiment was repeated three times. The data were proceeded by statistical analysis.

2.6. Mitochondrial membrane potential (MMP) assay

A mitochondrial-specific cationic dye (JC-1) was used for the assay. When the membrane potential is low, JC-1, as a monomer, emits green excitation light. At higher membrane potentials, JC-1 aggregates increase and emit red light. N2a cells were seeded in 6-well plates. After treatment at different concentrations for 3 h, JC-1 was added, incubated at 37 °C for 30 min, and then washed three times with JC-1 buffer. Then, the cell ratio of red and green fluorescence was measured by flow cytometry (FACS-Calibur, BD). The percentage of cells with reduced MMP among 30,000 cells was calculated. The data were proceeded by statistical analysis.

2.7. Western blotting

Protein content was determined in lysates of N2a cells that had been treated with PQ for different time intervals or NAC. The cells were washed three times with cold PBS, and RIPA lysis buffer containing 0.1% PMSF, 0.1% phosphatase inhibitor cocktail (MCE), and 0.1% protease inhibitor cocktail (MCE) was added on ice for 20 min. The supernatant was collected by centrifugation at 12,000 g for 15 min. The protein concentration was measured by the BCA method. Loading buffer was added. The protein samples (20–50 μ g) were separated by SDS-PAGE and transferred to PVDF membranes. The membranes were incubated with 5% skim milk powder or 2% BSA (for phosphorylated protein) for 1 h, followed by incubation with primary antibody overnight (4 °C). After washing 6 times (5 min each time), the membranes were incubated with HRP-conjugated antibody for 1 h at room temperature, washed 6 times (5 min each time), and then detected by an enhanced chemiluminescence kit. ImageJ software was used for densitometry of the protein bands. The ratio of the target protein signal to that of the corresponding internal reference gene (GAPDH) was the relative expression of each group of target genes. Then, the fold change of the treatment group was calculated. Finally, statistical analysis was performed.

2.8. MitoTracker and LysoTracker labeling

MitoTracker stock solution (1 mM) was diluted to the final

working concentration (200 nM) in growth medium. LysoTracker Red DND-99 stock solution (1 mM) was diluted to the final working concentration (100 nM) in growth medium. Cells were grown on coverslips inside Petri dishes filled with culture medium. When cells reached the desired confluency (50%), the media was removed from the dish, MitoTracker (200 nM) and LysoTracker Red DND-99 (100 nM) were added to the cultured primary mouse neurons or N2a cells, and the cells were placed in an incubator (37 °C) for 30 min. Then, the dye-containing medium was discarded, and the cells were washed with warm complete DMEM. Live cell real-time imaging was performed immediately with the Leica multiphoton system. The excitation and emission wavelengths of each fluorophore (588 nm and 647 nm) were selected according to the manufacturer's instructions (M22426, L7528). Red light (647 nm) was set to pseudocolor green on the confocal microscope system. When mitochondria are wrapped by lysosomes, red light and green light overlap to form yellow light. The numbers of yellow puncta were quantified with ImageJ. All data were analyzed in at least three repeated experiments. For neurons/cells in each group, at least 40 neurons were imaged through 3–4 different experiments. The MINA plug-in in ImageJ software was used to quantify mitochondrial length.

2.9. Mito-keima fluorescence

The lentiviral vector (COX8-mKeima) was synthesized by GenePharma (Shanghai, China). N2a cells were transfected with COX8-mKeima, and puromycin (0.6 μ g/ml, Sigma) was added to select positive cells. Cells (mt-Keima) were excited in 2 channels by 2 continuous wavelengths (458 nm, green; 561 nm, red) and measured. The labeled cells were imaged with a Leica multiphoton system. When mitochondria are wrapped by lysosomes, red light is increased and green light is decreased. The intensity of light was quantified with ImageJ. All experiments were repeated at least three times independently. In total, more than 40 neuronal cells were imaged.

2.10. Transmission electron microscope

After trypsin digestion, the cell samples were centrifuged and then 3% glutaraldehyde, and 1.5% paraformaldehyde were added to the samples and fixed at 4 °C for one day. The cell samples were washed with PBS three times followed by gradient dehydration, embedding, and finally ultrathin sectioning to obtain samples that could be employed for electron microscope observation. The mitochondrial morphology and mitophagy ultrastructure were visualized by transmission electron microscopy. ImageJ was used to quantify the percentage of damaged mitochondria and mitophagy events in the different groups.

2.11. DRP1 siRNA transfection

Three pairs of siRNAs (Table S1) at different sites (828, 1196, 1522) on DRP1 DNA were synthesized by GenePharma (Shanghai, China). Western blot verified the knockdown effect of DRP1. DRP1 protein decreased significantly, and the knockdown effect was better in the siDRP1-828 group (Fig. S6). When N2a cells reached 50%–60% confluence in the culture dish, the medium was discarded, new medium was added (2 ml), and 5 μ L of premixed siRNA (50 nM) and 5 μ L of siRNA-Mate plus siRNA were added. After 6 h, PQ (200 μ M) was added to the PQ treatment group for 3 h. Then, MitoTracker (200 nM, 20 min) was added, and the culture medium was discarded and washed with PBS. Mitochondria were photographed by laser confocal scanning microscopy.

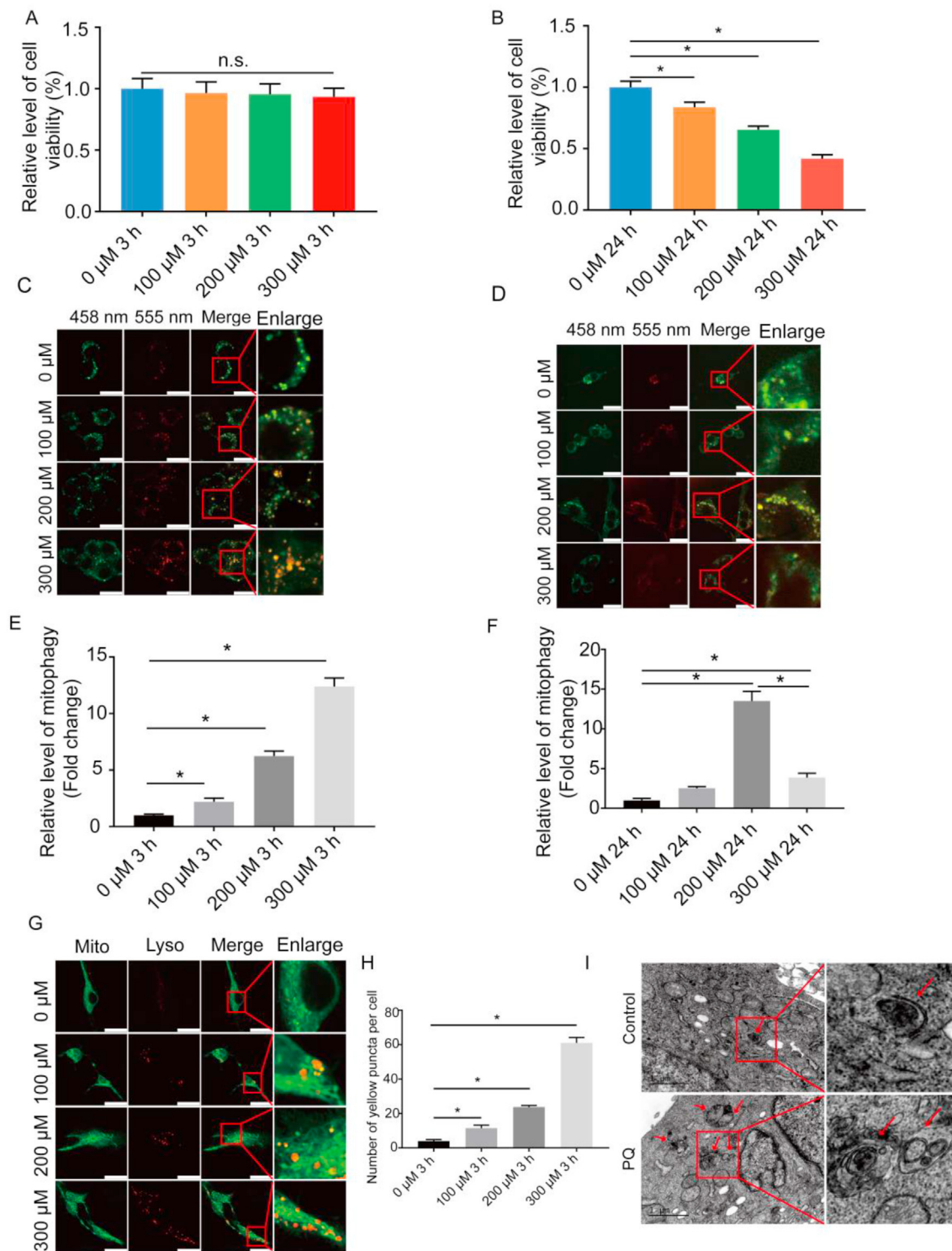


Fig. 1. Gradient PQ treatment of neuronal cells can significantly enhance mitophagy. (A) The cell viability was determined of N2a cells treated with gradient concentrations (0–300 μ M) of PQ for 3 h. (B) The viability of N2a cells treated with gradient concentrations (100–300 μ M) of PQ for 24 h is shown. (C) The level of mitophagy was assessed after PQ treatment of N2a cells for 3 h. The relative level of mitophagy is shown in (E). The white line in the lower right corner represents the scale. Scale bar = 25 μ m. (D) The level of mitophagy was determined in N2a cells treated with 0, 100, 200, or 300 μ M PQ for 24 h. The relative level of mitophagy is shown in (F). The white line in the lower right corner represents the scale. Scale bar = 25 μ m. (G) The level of mitophagy was determined in primary neurons treated with 0, 100, 200, or 300 μ M PQ for 3 h. The white line in the lower right corner represents the scale. Scale bar = 25 μ m. The relative level of mitophagy is shown in (I). (H) Transmission electron microscopy was used to detect the ultrastructure of mitochondrial autophagosomes (red arrows indicate mitochondrial autophagosomes) after 200 μ M PQ treatment of N2a cells for 3 h. Scale bar = 1 μ m. (n = 3; * indicates comparison between the two groups $P < 0.05$). (For interpretation of the references to color in this figure legend, the reader is referred to the Web version of this article.)

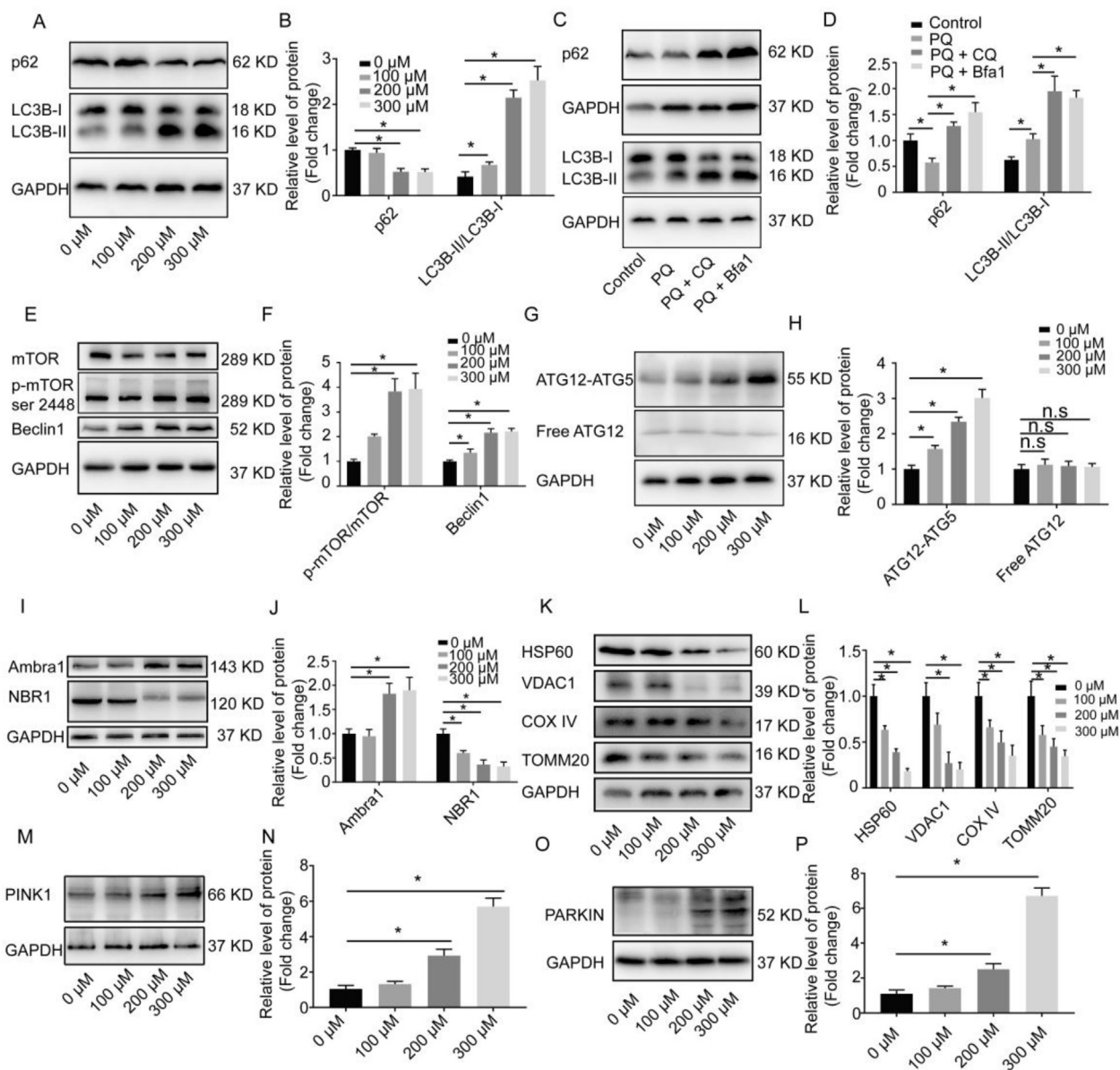


Fig. 2. PQ treatment of neuronal cells can significantly activate the mitochondrial autophagy pathway. (A) Autophagy marker protein LC3B and p62 levels were analyzed after N2a cells were treated with gradient concentrations (100–300 μM) of PQs for 3 h. (B) Statistical analysis of LC3B and p62 levels is shown. (C, D) The relative levels of the autophagy marker proteins LC3B and p62 are shown. After blocking the degradation of autophagosomes with chloroquine (CQ) and bafilomycin A1 (Bfa1), N2a cells were treated with 200 μM PQ for 3 h. (E, F) The levels of the autophagy pathway proteins p-mTOR and Beclin1 are shown. (G, H) The levels of autophagy pathway proteins ATG12 and ATG12-ATG5 are shown. (I, J) The levels of autophagy pathway proteins Ambra1 and NBR1 are shown. (K, L) The levels of mitochondrial proteins HSP60, VDAC1, COX IV, and TOMM20 are shown. (M, N) The level of mitophagy marker protein PINK1 is shown. (O, P) The level of PARKIN is shown in N2a cells after treatment with gradient concentrations (0–300 μM) of PQ for 3 h (n = 3; * indicates comparison between the two groups P < 0.05).

2.12. Immunofluorescence experiment

N2a cells were treated with 0–300 μM paraquat for 3 h. The culture medium was discarded, and the cells were washed with PBS. Then, the cells were fixed with 4% paraformaldehyde for 10 min, and the cell membranes were permeated with 0.1% Triton-100 for 10 min. Then, the cells were blocked with 1% BSA for 1 h. The primary antibody (TOMM20: 1/500; PINK1: 1/300; PARKIN: 1/300) was added and incubated overnight at 4 °C. After washing with PBS 3 times, fluorescent secondary antibody (488 nm, 647 nm) was added and incubated for 1 h at room temperature. Finally, 1 μg/ml of DAPI was added and incubated for 15 min. Then, the samples were photographed by laser confocal microscopy.

2.13. Statistical analysis

SPSS 19.0 was used for statistical analysis. The data are shown as the mean ± standard deviation (SD). First, one-way ANOVA was used to analyze the comparison of multiple groups of data. After conducting significant ANOVAs, Bonferroni post hoc test or Tukey post hoc test was used for multiple comparisons. P < 0.05 was considered statistically significant. All graphics were produced using GraphPad Prism (GraphPad software, San Diego, California, CA, USA).

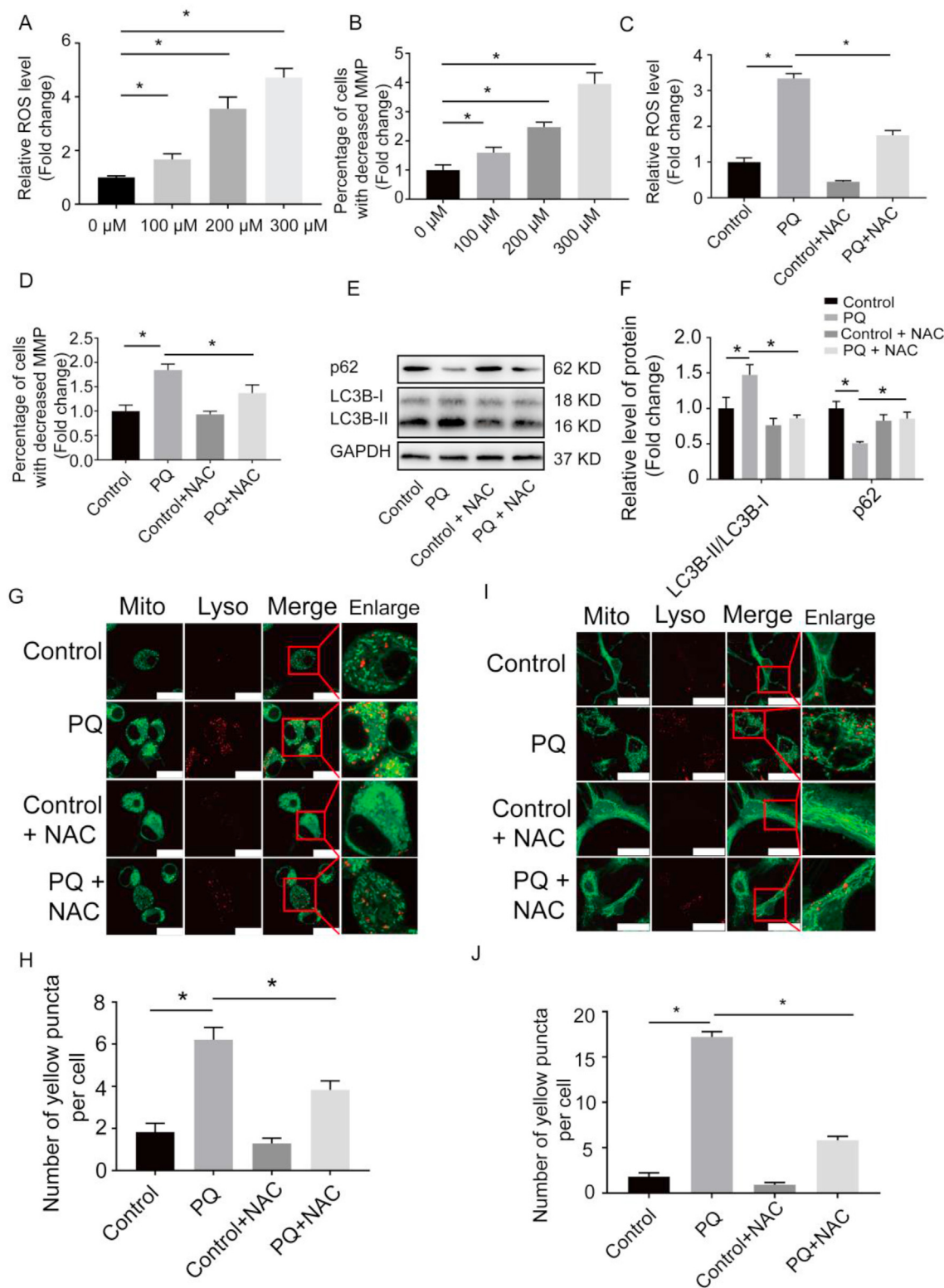
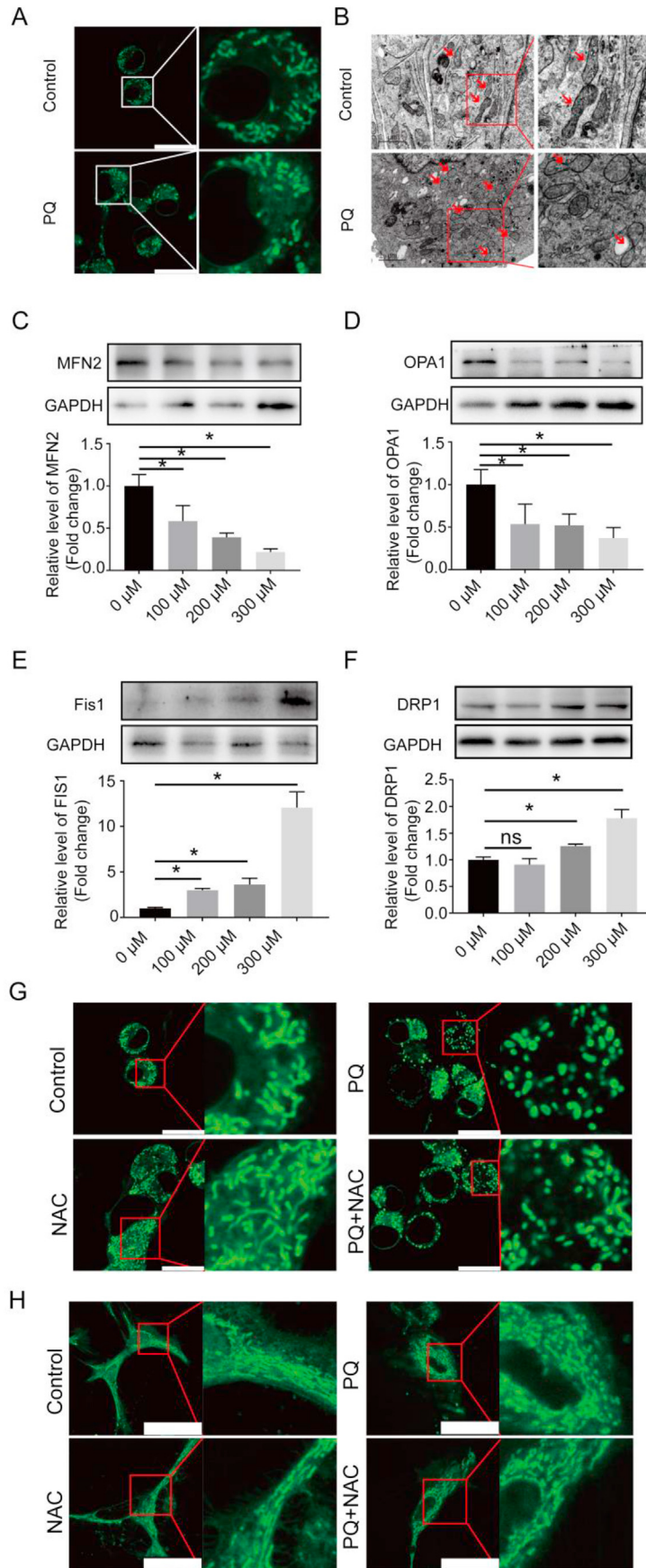


Fig. 3. ROS are a key signaling factor for PQ-induced mitophagy. (A) The relative number of cells with increased ROS was determined. The amount of ROS produced by N2a cells induced by gradient concentrations of PQ for 3 h is shown. (B) The relative number of cells with reduced MMP was determined. The relative number of cells with reduced MMP in each group was analyzed. (C) The relative number of cells with increased ROS was determined. N2a cells were pretreated with 10 μ M NAC, and then PQ was added for 3 h. (D) The relative number of cells with reduced MMP. N2a cells were pretreated with 10 μ M NAC and then treated with PQ for 3 h. (E, F) The levels of the autophagy marker proteins LC3B and p62 are shown. N2a cells were pretreated with 10 μ M NAC and treated with PQ for 3 h. (G, H) The level of mitophagy in N2a cells was determined. N2a cells were pretreated with 10 μ M NAC, and PQ was added for 3 h. The white line in the lower right corner represents the scale. Scale bar = 25 μ m. (I, J) The relative level of mitophagy in primary neuronal cells was determined. Primary neuronal cells of mice were pretreated with 10 μ M NAC, and then PQ was added for 3 h. The white line in the lower right corner represents the scale. Scale bar = 25 μ m. (n = 3; * indicates comparison between the two groups $P < 0.05$).



3. Results

3.1. Mitophagy was enhanced in the process of paraquat-induced neuronal cell damage

In this experiment, N2a cells were treated with 0–300 μM PQ for 3, 6, 12, and 24 h. The results showed that cell viability did not decrease significantly with a treatment time of 3 h (Fig. 1A). Cell viability was decreased significantly in the 300 μM group after 6 and 12 h of treatment (Figs. S1A and B). Cell viability was reduced to 83.7%, 55.4% and 41.9% in N2a cells that were treated with different concentrations (100, 200 and 300 μM) of PQ for 24 h, respectively (Fig. 1B). Additionally, N2a cells (COX8-mkemia expression stable) were treated with 0, 100, 200, and 300 μM PQ for 3, 6, 12, and 24 h. Red light was increased, and green light was decreased. This result indicated that mitophagy increased significantly (Fig. 1C, D, E, F and Figs. S1C and D). Interestingly, mitophagy was significantly lower in the 300 μM PQ group than in the 200 μM PQ group after 24 h of treatment (Fig. 1D). Additionally, primary neuronal cells were used to verify the results that PQ promoted mitophagy. Primary neuronal cells were treated with gradient concentrations of PQ (100–300 μM) for 3 h. The results showed that mitophagy was increased significantly (Fig. 1G and H). To confirm that PQ promoted mitophagy in a short time, the level of mitochondrial autophagosomes was detected by transmission electron scanning microscopy in N2a cells after 200 μM PQ exposure for 3 h. The results showed that the mitochondrial autophagosomes increased significantly after 200 μM PQ treatment for 3 h in N2a cells (Fig. 1I).

3.2. Acute exposure to PQ significantly activates the key signals of the mitochondrial autophagy pathway

To understand the underlying mechanism of PQ in neuronal mitophagy, we examined the changes in key proteins in the autophagy pathway and the levels of mitochondrial proteins. Our results showed that the LC3B-II/LC3B-I ratio was significantly increased, and P62 was significantly decreased after 100, 200, 300 μM PQ treatment for 3 h in N2a cells (Fig. 2A and B). To further confirm that autophagy was promoted by PQ in neural cells, the autophagy inhibitors chloroquine (CQ) and bafilomycin A1 (Bfa1) were used to block autophagic degradation. The results showed that the p62 and LC3B-II/LC3B-I levels were more significantly increased when autophagy was blocked by chloroquine and bafilomycin in N2a cells (Fig. 2C and D). Additionally, key proteins of autophagy signaling pathways were detected in N2a cells after 0–300 μM PQ treatment for 3 h. The results showed that the levels of p-mTOR/mTOR and Beclin1 in the autophagy induction phase and the vesicle nucleation phase increased significantly (Fig. 2E and F). The ATG12-ATG5 complex in the autophagosome extension phase pathway was significantly increased. Nevertheless, the ATG12 monomer level was not significantly changed (Fig. 2G and H), Ambra1 was significantly increased, and the NBR1 level was significantly reduced (Fig. 2I and J). The mitophagy-related proteins PINK1 and PARKIN were significantly increased (Fig. 2O, P). PINK1 and PARKIN were enriched in mitochondria during PQ treatment (Figs. S2C and D). Mitochondrial mass marker protein levels were examined in N2a cells under 0, 100, 200, and 300 μM PQ treatment

for 3 h. The results showed that HSP60, VDAC1, COX IV, and TOMM20 were decreased significantly (Fig. 2K and L).

3.3. The decrease in MMP caused by increased ROS was an important factor in enhancing mitophagy induced by PQ

Our study showed that ROS were increased significantly after 100, 200, and 300 μM PQ treatment for 3 h in N2a cells (Fig. 3A and Fig. S3A), and the percentage of cells with reduced MMP was increased significantly (Fig. 3B and Fig. S3C). To determine the role of ROS in the process of MMP reduction caused by PQ, we added NAC. The experimental results showed that intracellular ROS, which was induced by PQ, was significantly decreased by NAC (Fig. 3C and Fig. S3B). Furthermore, the percentage of cells with reduced MMP, which was increased by PQ, was partially restored by NAC (Fig. 3D and Fig. S3D). On this basis, the level of mitophagy, which was induced by PQ, was detected after NAC addition. The experimental results showed that increasing LC3B-II/LC3B-I and decreasing P62 were rescued by NAC (Fig. 3E and F). Further experiments showed that the increase in mitophagy caused by PQ was partially reversed by NAC in N2a cells (Fig. 3G and H) or primary neuronal cells (Fig. 3I and J).

3.4. ROS promote mitochondrial fission and enhance the neurotoxicity of paraquat

Previous studies have suggested that mitochondrial fission and fusion play an important role in mitophagy (Chen and Chan, 2009; Chen et al., 2016; Martinez et al., 2018). Our results showed that mitochondrial fission was enhanced, and the number of short round mitochondria was increased significantly with 200 μM PQ treatment for 3 h in N2a cells (Fig. 4A and B and Fig. S4A). Key proteins involved in mitochondrial fission and fusion were detected. The results showed that MFN2 and OPA1 were significantly reduced after 100, 200, 300 μM PQ treatment for 3 h (Fig. 4C and D). FIS1 and DRP1 were significantly increased (Fig. 4E and F). Previous studies have found that oxidative stress is one of the main mechanisms of paraquat neurotoxicity. Our experimental results also showed that mitochondrial fission, which was enhanced by PQ, was reversed by NAC in N2a cells or primary neuronal cells (Fig. 4G and H). Mitochondrial length, which was reduced by PQ, was reversed by NAC in N2a cells or primary neuronal cells (Figs. S4B and C).

3.5. The role of DRP1-mediated mitochondrial fission in PQ-induced mitophagy in N2a cells

In this study, we pretreated N2a cells with 10 μM mdivi-1 (a DRP1 inhibitor) for 2 h or DRP1 siRNA, followed by 200 μM PQ treatment for 3 h. MitoTracker-labeled mitochondria were examined by laser confocal scanning microscopy. The results showed that mitochondrial fission was increased in the PQ treatment group, while the number of fragmented mitochondria was reduced when DRP1 was inhibited or knocked down (Fig. 5A and B and Figs. S4D and E). Mitochondrial morphology was detected by transmission electron microscopy in the same model, and the results were consistent with the results of laser confocal microscopy (Fig. 5C). The level of mitophagy was detected when DRP1 was inhibited by

Fig. 4. ROS are key signaling factors that significantly increase mitochondrial fission in N2a cells caused by PQ exposure. (A) Mitochondrial fission and fusion were assessed in N2a cells treated with 200 μM PQ for 3 h. The white line in the lower right corner represents the scale. Scale bar = 20 μm . (B) The ultrastructure is shown of mitochondria after N2a cells were treated with 200 μM PQ for 3 h (red arrows indicate mitochondria). Scale bar = 1 μm . (C, D, E, F) The levels of key mitochondrial fusion proteins MFN2, OPA1, FIS1 and DRP1 are shown. (G) The mitochondrial fission and fusion status was determined in N2a cells that were pretreated with 10 μM NAC and treated with PQ for 3 h. The white line in the lower right corner represents the scale. Scale bar = 20 μm . (H) The mitochondrial fission and fusion status was determined in primary neuronal cells that were pretreated with 10 μM NAC and treated with PQ for 3 h. The white line in the lower right corner represents the scale. Scale bar = 25 μm . (n = 3; * indicates comparison between the two groups $P < 0.05$). (For interpretation of the references to color in this figure legend, the reader is referred to the Web version of this article.)

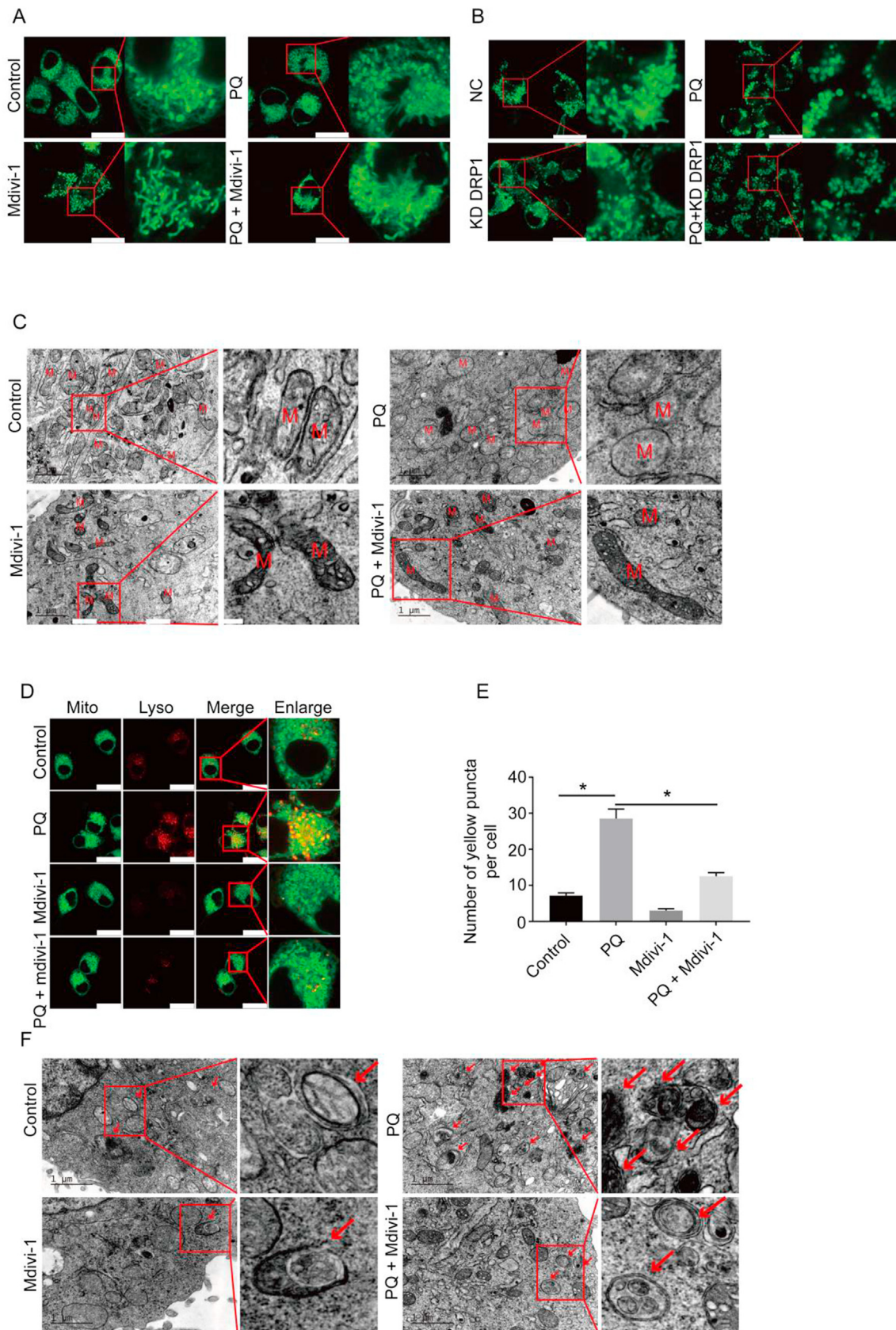


Fig. 5. DRP1-mediated mitochondrial fission contributes to PQ-induced mitophagy in N2a cells. (A) The mitochondrial status was assessed in N2a cells that were pretreated with mdivi-1 and treated with 200 μ M PQ for 3 h. The white line in the lower right corner represents the scale. Scale bar = 20 μ m. (B) The mitochondrial status was assessed in N2a cells that were pretreated with siRNA and treated with 200 μ M PQ for 3 h. The white line in the lower right corner represents the scale. Scale bar = 20 μ m. (C) The ultrastructure of mitochondria in N2a cells pretreated with mdivi-1 and treated with 200 μ M PQ for 3 h is shown (red arrows indicate mitochondria); scale bar = 1 μ m. (D, E) The relative level of

mdivi-1. The results showed that the enhancement of mitophagy, which was induced by PQ, was rescued by mdivi-1 (Fig. 5D and E). The level of mitophagy was also detected by transmission electron microscopy in the same treatment model. The results were consistent with the laser confocal scanning microscopy results (Fig. 5F). This result suggested that inhibition of mitochondrial fission could rescue the enhancement of mitophagy caused by PQ treatment.

4. Discussion

The study provided evidence of the role and mechanism of mitophagy in the neurological damage caused by PQ. Our results showed that 100, 200, and 300 μM PQ induced mitophagy in a dose-dependent manner in neuronal cells. Mitochondrial fission was enhanced by 100, 200 and 300 μM PQ in neuronal cells. Moreover, mitochondrial fission and mitophagy were enhanced at least during the first 12 h of exposure. Our results also suggested that the decreased MMP and increased ROS might contribute to the enhancement of mitophagy caused by PQ. In particular, our results showed that DRP1-mediated mitochondrial fission was involved in neuronal mitophagy enhancement caused by PQ.

Our results showed that 100, 200, and 300 μM PQ could significantly promote neuronal mitophagy at 3, 6, 12, or 24 h. Consistent with previous reports (Liu et al., 2020; Ramirez-Moreno et al., 2019; Wang and Miller, 2012), a significant increase in mitophagy was observed in N2a cells and primary neurons treated with PQ in our study. Although mitophagy was supported by the results, the 6 h PQ treatment induced a lower level of relative mitophagy than the 3 h treatment. In addition, the relative mitophagy level with 100 μM PQ for the 24 h treatment time was lower than that at shorter treatment times. When we designed the experiment, 3, 6, 12, and 24 h were operated separately. This might have influenced the comparison between different time points. Therefore, comparisons between different time points need to be performed with caution. In future studies, a different dose time period could be designed to facilitate the comparison of different times. In our study, cell viability was reduced in N2a cells treated with different concentrations (100, 200 and 300 μM) of PQ for 24 h. A physiologically based pharmacokinetic (PBPK) model showed that the PQ burden in the brain accumulated gradually with increasing age within a lifetime PQ exposure scenario. Furthermore, people ≥ 50 years of age had significantly higher PQ exposure risks with PQ burden estimates of 424.79 μM (Cheng et al., 2018). However, the experimental results should be extrapolated with caution due to differences in vivo and in vitro and exposure time differences. It is not possible to directly compare the PQ concentration used in this study with the 400 μM concentration in previous reports. Furthermore, our results showed that the key proteins of the pathway in the stages of autophagy induction, autophagy nucleation, and autophagosome extension were activated by PQ. The results provided evidence that the neuron autophagy pathway was activated by PQ at concentrations as low as 100 μM for 3 h.

Interestingly, an unanticipated result was noticed in 24 h PQ treatment tests. The results showed that mitophagy was reduced in the 300 μM PQ group compared with the 200 μM group. The possible reasons are as follows. One possible reason was that cell death was caused by excessive mitophagy. The second possible reason was that the mitophagy pathway was damaged by PQ, and

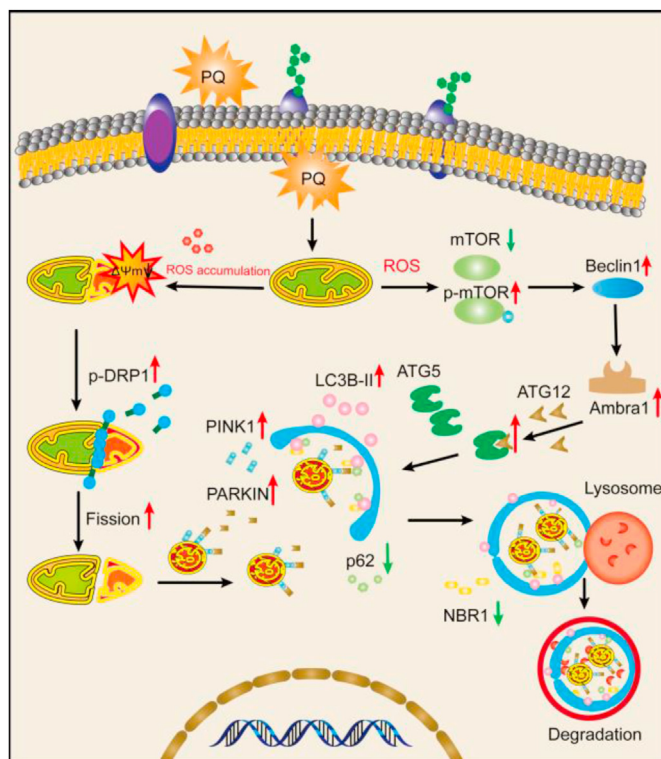


Fig. 6. Schematic representation of excessive mitophagy induced by low-concentration PQ administration in neuronal cells. In this study, we showed that less than 100 μM PQ activated autophagy signaling through ROS and increased downstream regulator expression in neuronal cells. The following results verified significant phosphorylation of DRP1 in PQ-treated N2a cells, which was consistent with the function of DRP1 documented in previous articles. To further gain insight into the relationship between DRP1 and mitophagy, we blocked DRP1 and found that increases in mitochondrial fission and mitophagy were attenuated by mdivi-1. Collectively, these results suggest that DRP1-mediated mitochondrial fission contributes to PQ-induced excessive mitophagy.

mitophagy was decreased at this concentration and incubation period. Therefore, chloroquine was used to block the degradation of autophagy in a system with 300 μM PQ for 24 h, and then autophagic flow was detected. The results showed that the autophagy marker protein LC3B-II was increased further after treatment with 300 μM PQ for 24 h (Fig. S2 A, B). Therefore, our results might indicate that there are PQ-induced (300 μM , 24 h) decreases in the number of autophagosomes, owing to excessive autophagy rather than a disruption of autophagy. Excessive autophagy might cause cell death (Cao et al., 2019b; Pellacani and Costa, 2018). The third possible reason was that apoptosis was significantly increased and cell viability was decreased under this condition. Our previous results showed that apoptosis was significantly increased in N2a cells after 300 μM paraquat treatment for 24 h (Yang et al., 2020). All of these findings might provide a possible explanation for the death of dopamine neurons caused by long-term exposure to low concentrations of PQ.

ROS are responsible for the neurotoxicity of PQ treatment in mammals (Li et al., 2012; Musgrove et al., 2019). Notably, under our working conditions, short-term exposure to low-concentration PQ caused an obvious increase in ROS and a decrease in MMP. Removal

mitophagy was assessed in N2a cells pretreated with mdivi-1 and treated with 200 μM PQ for 3 h. The white line in the lower right corner represents the scale. Scale bar = 20 μm . (F) The ultrastructure of mitophagy was assessed in N2a cells that were pretreated with mdivi-1 and treated with 200 μM PQ for 3 h (red arrows indicate mitochondrial autophagosomes); scale bar = 1 μm . (n = 3; *indicates comparison between the two groups $P < 0.05$). (For interpretation of the references to color in this figure legend, the reader is referred to the Web version of this article.)

of ROS reversed the decrease in MMP and the increased mitophagy caused by PQ treatment, suggesting that ROS may be linked to PQ exposure to intermediate variables with enhanced neuronal mitophagy. This observation was consistent with the notion that ROS-induced MMP operates as a major reason for mitophagy upon exposure to PQ (Liu et al., 2020; Sun et al., 2018). Furthermore, PQ-induced cytotoxicity focusing on MMP, which has been implicated in neurodegeneration, was investigated (Huang et al., 2016). However, the potential mechanism by which ROS enhance mitophagy in neurons is not fully clear. ROS generation during cell stress might be the origin of mitochondrial fission. The possibility of ROS promoting Drp1-mediated mitochondrial fission in mitophagy was considered.

Once proven that PQ-induced MMP decreases and promotes mitophagy, we wished to gain insight into the mechanisms involved herein. Our study showed that mitochondrial fission was increased significantly, and the number of short round mitochondria was increased after treating neurons with 200 μ M PQ for 3 h. Our results also showed that the levels of mitochondrial fission-related proteins DRP1 and FIS1 were increased significantly, and mitochondrial fusion-related proteins MFN2 and OPA1 were decreased significantly under 100 μ M PQ treatment for a short time (3 h) in neuronal cells. Our results also showed that removal of ROS by NAC partially reversed the enhanced mitochondrial fission caused by PQ treatment; short round mitochondria were reduced, and long mitochondria were increased. Our data indicated that mitochondrial quality control played a role in the neurotoxicity caused by PQ. Zhao et al. (2017) described the relationships among PQ, ROS production, and mitochondrial fission. PQ broke down the mitochondrial network, enhanced the expression of fission-related proteins, and increased Drp1 in AT II cells that were treated with different concentrations (200, 400, 800 and 1600 μ M) of PQ for 24 h (Zhao et al., 2017). Mitochondrial quality control refers to the process by which mitochondrial morphology, length, size, quantity, and quality are strictly regulated and maintain the distribution and function of mitochondria (Stotland and Gottlieb, 2015). This process is precisely regulated by the dynamic balance of mitochondrial fusion and fission. Mitochondria do not exist entirely in a free, single form in the body but form a dynamically changing network structure (Chen and Chan, 2005). Mitochondrial fusion and fission play an important role in mitophagy, and the steady-state imbalance of fission-fusion dynamic balance is an important cause of mitophagy (Ge et al., 2020). Mitophagy digests and clears small, elliptical mitochondria, while elongated mitochondria are protected from autophagic degradation and maintain ATP levels (Alaimo et al., 2019; Gomes et al., 2011). Therefore, mitochondrial fission might be a necessary condition for mitophagy.

Additionally, DRP1 is a key regulator that mediates the dynamic balance of cell mitochondrial fission-fusion (Bereiter-Hahn and Jendrach, 2010; Zhang et al., 2016). Since DRP1 is known to be an important fission signal in the toxicological effect of PQ, we hypothesized that treatment with mdivi-1 (a DRP1 inhibitor) would rescue mitophagy flux in cells suffering from PQ. Our results showed that mitophagy was diminished by mdivi-1 pretreatment in PQ-challenged cultures. Although increasing evidence has shown that Drp1 is required for mitophagy in mammalian cells (Anding et al., 2018; Ikeda et al., 2015; Reddy and Oliver, 2019), limited research has also reported that Drp1 is not required for mitophagy in mammalian cells (Han et al., 2020; Song et al., 2015). Therefore, whether Drp1-mediated mitochondrial fission has an important role in mitophagy remains controversial. Our results provide evidence that mitochondrial fission is necessary for mitophagy to occur in PQ-treated neural cells.

5. Conclusion

In conclusion, this study presents compelling evidence that short-term exposure to PQ could activate autophagy signaling and mitochondrial fission through ROS in neuronal cells. Moreover, activation of the ROS signaling pathway and the formation of DRP1 regulation were demonstrated to play a prominent role in PQ-induced mitophagy (Fig. 6). Altogether, our findings provide new insight into the toxic mechanisms underlying PQ-triggered mitophagy and mitochondrial fission and imply that DRP1-mediated mitochondrial fission in neurons could be an alternative target for the prevention and treatment of PQ-induced excessive mitophagy in neural cells.

Funding

This work was supported by the National Natural Science Foundation of China under Grant (No. 81573195, 81973083, 81903352 and 81601144); the Joint Funds for the Innovation of Science and Technology, Fujian province (No. 2017Y9105); and the Fujian Medical University Startup Fund (XRCZX2019007); the Sailing Funding of Fujian Medical University (2017XQ 2012; 2018QH1009).

Declaration of competing interest

The authors declare that they have no known competing financial interests or personal relationships that could have appeared to influence the work reported in this paper.

Acknowledgements

The authors would like to thank Nan Ren, Lingfen Luo, Jinfa Chen, and Xinan Wen from The Experimental Centre of School of Public Health (Fujian Medical University, Fuzhou, China) for their technical assistance. The authors also would like to thank Junjin Lin, Ling Lin, linyin Zhou, and Shuping Zeng from the Public Technology Service Center (Fujian Medical University, Fuzhou, China) for their technical assistance.

Appendix A. Supplementary data

Supplementary data to this article can be found online at <https://doi.org/10.1016/j.envpol.2020.116413>.

References

- Alaimo, A., Liñares, G.G., Bujjamer, J.M., Gorojod, R.M., Alcon, S.P., Martínez, J.H., Baldessari, A., Grecco, H.E., Kotler, M.L., 2019. Toxicity of blue led light and A2E is associated to mitochondrial dynamics impairment in ARPE-19 cells: implications for age-related macular degeneration. *Arch. Toxicol.* 93, 1401–1415. <https://doi.org/10.1007/s00204-019-02409-6>.
- Amondham, W., Parkpian, P., Polprasert, C., DeLaune, R., Jugsujinda, A., 2006. Paraquat adsorption, degradation, and remobilization in tropical soils of Thailand. *J. Environ. Sci. Health Part B Pestic. Food Contam. Agric. Wastes* 41, 485–507. <https://doi.org/10.1080/03601230600701635>.
- Anding, A.L., Wang, C., Chang, T.-K., Sliter, D.A., Powers, C.M., Hofmann, K., Youle, R.J., Baehrecke, E.H., 2018. Vps13D encodes a ubiquitin-binding protein that is required for the regulation of mitochondrial size and clearance. *Curr. Biol.* 28, 287–295. <https://doi.org/10.1016/j.cub.2017.11.064>.
- Baltazar, M.T., Dinis-Oliveira, R.J., de Lourdes Bastos, M., Tsatsakis, A.M., Duarte, J.A., Carvalho, F., 2014. Pesticides exposure as etiological factors of Parkinson's disease and other neurodegenerative diseases—A mechanistic approach. *Toxicol. Lett.* 230, 85–103. <https://doi.org/10.1016/j.toxlet.2014.01.039>.
- Bereiter-Hahn, J., Jendrach, M., 2010. Mitochondrial dynamics. *Int Rev Cell Mol Biol* 1–65. [https://doi.org/10.1016/S1937-6448\(10\)84001-8](https://doi.org/10.1016/S1937-6448(10)84001-8).
- Bingol, B., Tea, J.S., Phu, L., Reichelt, M., Bakalarski, C.E., Song, Q., Foreman, O., Kirkpatrick, D.S., Sheng, M., 2014. The mitochondrial deubiquitinase USP30 opposes parkin-mediated mitophagy. *Nature* 510, 370–375. <https://doi.org/10.1038/nature13418>.

- Bonello, F., Hassoun, S.-M., Mouton-Liger, F., Shin, Y.S., Muscat, A., Tesson, C., Lesage, S., Beart, P.M., Brice, A., Krupp, J., Corvol, J.-C., Corti, O., 2019. LRRK2 impairs PINK1/Parkin-dependent mitophagy via its kinase activity: pathologic insights into Parkinson's disease. *Hum. Mol. Genet.* 28, 1645–1660. <https://doi.org/10.1093/hmg/ddz004>.
- Bose, A., Beal, M.F., 2019. Mitochondrial dysfunction and oxidative stress in induced pluripotent stem cell models of Parkinson's disease. *Eur. J. Neurosci.* 49, 525–532. <https://doi.org/10.1111/ejn.14264>.
- Bose, A., Beal, M.F., 2016. Mitochondrial dysfunction in Parkinson's disease. *J. Neurochem.* 139, 216–231. <https://doi.org/10.1111/jnc.13731>.
- Cai, Z., Zheng, F., Ding, Y., Zhan, Y., Gong, R., Li, J., Aschner, M., Zhang, Q., Wu, S., Li, H., 2019. Nrf2-regulated miR-380-3p blocks the translation of Sp3 protein and its mediation of paraquat-induced toxicity in mouse neuroblastoma N2a cells. *Toxicol. Sci.* 171, 515–529. <https://doi.org/10.1093/toxsci/kfz162>.
- Cao, F., Souders II, C.L., Perez-Rodriguez, V., Martyniuk, C.J., 2019a. Elucidating conserved transcriptional networks underlying pesticide exposure and Parkinson's disease: a focus on chemicals of epidemiological relevance. *Front. Genet.* 9 <https://doi.org/10.3389/fgene.2018.00701>.
- Cao, Y., Li, Qinglin, Liu, L., Wu, H., Huang, F., Wang, C., Lan, Y., Zheng, F., Xing, F., Zhou, Q., Li, Qi, Shi, H., Zhang, B., Wang, Z., Wu, X., 2019b. Modafinil protects hippocampal neurons by suppressing excessive autophagy and apoptosis in mice with sleep deprivation. *Br. J. Pharmacol.* 176, 1282–1297. <https://doi.org/10.1111/bph.14626>.
- Chen, H., Chan, D.C., 2009. Mitochondrial dynamics-fusion, fission, movement, and mitophagy-in neurodegenerative diseases. *Hum. Mol. Genet.* 18, 169–176. <https://doi.org/10.1093/hmg/ddp326>.
- Chen, H., Chan, D.C., 2005. Emerging functions of mammalian mitochondrial fusion and fission. *Hum. Mol. Genet.* 14, R283–R289. <https://doi.org/10.1093/hmg/ddi270>.
- Chen, M., Chen, Z., Wang, Y., Tan, Z., Zhu, C., Li, Y., Han, Z., Chen, L., Gao, R., Liu, L., Chen, Q., 2016. Mitophagy receptor FUNDC1 regulates mitochondrial dynamics and mitophagy. *Autophagy* 12, 689–702. <https://doi.org/10.1080/15548627.2016.1151580>.
- Chen, Z., Liu, L., Cheng, Q., Li, Y., Wu, H., Zhang, W., Wang, Y., Sehgal, S.A., Siraj, S., Wang, X., Wang, J., Zhu, Y., Chen, Q., 2017. Mitochondrial E3 ligase MARCH5 regulates FUNDC1 to fine-tune hypoxic mitophagy. *EMBO Rep.* 18, 495–509. <https://doi.org/10.15252/embr.201643309>.
- Cheng, Y.H., Chou, W.C., Yang, Y.F., Huang, C.W., How, C.M., Chen, S.C., Chen, W.Y., Hsieh, N.H., Lin, Y.J., You, S.H., Liao, C.M., 2018. PBPK/PD assessment for Parkinson's disease risk posed by airborne pesticide paraquat exposure. *Environ. Sci. Pollut. Res.* 25, 5359–5368. <https://doi.org/10.1007/s11356-017-0875-4>.
- Chintia, S.J., Woods, G., Demaria, M., Rane, A., Zou, Y., McQuade, A., Rajagopalan, S., Limbad, C., Madden, D.T., Campisi, J., Andersen, J.K., 2018. Cellular senescence is induced by the environmental neurotoxin paraquat and contributes to neuropathology linked to Parkinson's disease. *Cell Rep.* 22, 930–940. <https://doi.org/10.1016/j.celrep.2017.12.092>.
- Chuang, J.L., Pan, L.L., Hsieh, C.Y., Huang, C.Y., Chen, P.C., Shin, J.W., 2016. Melatonin prevents the dynam-related protein 1-dependent mitochondrial fission and oxidative insult in the cortical neurons after 1-methyl-4-phenylpyridinium treatment. *J. Pineal Res.* 1, 230–240. <https://doi.org/10.1111/jpi.12343>.
- Filichia, E., Hoffer, B., Qi, X., Luo, Y., 2016. Inhibition of Drp1 mitochondrial translocation provides neural protection in dopaminergic system in a Parkinson's disease model induced by MPTP. *Sci. Rep.* 6, 1–13. <https://doi.org/10.1038/srep32656>.
- Friedman, J.H., 2019. Early- vs late-start levodopa relieved symptoms but did not affect disease progression in Parkinson disease. *Ann. Intern. Med.* 170, JC56. <https://doi.org/10.7326/ACP021905210-056>.
- Ge, P., Dawson, V.L., Dawson, T.M., 2020. PINK1 and Parkin mitochondrial quality control: a source of regional vulnerability in Parkinson's disease. *Mol. Neurodegener.* 15, 20. <https://doi.org/10.1186/s13024-020-00367-7>.
- Gomes, L.C., Benedetto, G. Di, Scorrano, L., 2011. During autophagy mitochondria elongate, are spared from degradation and sustain cell viability. *Nat. Cell Biol.* 13, 589–598. <https://doi.org/10.1038/ncb2220>.
- Han, H., Tan, J., Wang, R., Wan, H., He, Y., Yan, X., Guo, J., Gao, Q., Li, J., Shang, S., Chen, F., Tian, R., Liu, W., Liao, L., Tang, B., Zhang, Z., 2020. PINK1 phosphorylates Drp1 to regulate mitophagy-independent mitochondrial dynamics. *EMBO Rep.* 8, e48686 <https://doi.org/10.15252/embr.201948686>.
- Heckmann, B.L., Teubner, B.J.W., Tummers, B., Boada-Romero, E., Harris, L., Yang, M., Guy, C.S., Zakharenko, S.S., Green, D.R., 2019. LC3-Associated endocytosis facilitates β -amyloid clearance and mitigates neurodegeneration in murine Alzheimer's disease. *Cell* 178, 536–551. <https://doi.org/10.1016/j.cell.2019.05.056>.
- Huang, C.L., Chao, C.C., Lee, Y.C., Lu, M.K., Cheng, J.J., Yang, Y.C., Wang, V.C., Chang, W.C., Huang, N.K., 2016. Paraquat induces cell death through impairing mitochondrial membrane permeability. *Mol. Neurobiol.* 53, 2169–2188. <https://doi.org/10.1007/s12035-015-9198-y>.
- Ikeda, Y., Shirakabe, A., Maejima, Y., Zhai, P., Sciarretta, S., Toli, J., Nomura, M., Mihara, K., Egashira, K., Ohishi, M., Abdellatif, M., Sadoshima, J., 2015. Endogenous Drp1 mediates mitochondrial autophagy and protects the heart against energy stress. *Circ. Res.* 116, 264–278. <https://doi.org/10.1161/CIRCRESAHA.116.303356>.
- Kalia, L.V., Lang, A.E., 2015. Parkinson's disease. *Lancet* 386, 896–912. [https://doi.org/10.1016/S0140-6736\(14\)61393-3](https://doi.org/10.1016/S0140-6736(14)61393-3).
- Kamel, F., Tanner, C.M., Umbach, D.M., Hoppin, J.A., Alavanja, M.C.R., Blair, A., Comyns, K., Goldman, S.M., Korell, M., Langston, J.W., Ross, G.W., Sandler, D.P., 2007. Pesticide exposure and self-reported Parkinson's disease in the agricultural health study. *Am. J. Epidemiol.* 165, 364–374. <https://doi.org/10.1093/aje/kwk024>.
- Kang, R.R., Sun, Q., Chen, K.G., Cao, Q.T., Liu, C., Liu, K., Ma, Z., Deng, Y., Liu, W., Xu, B., 2020. Resveratrol Prevents Benzo(a)pyrene-Induced Disruption of Mitochondrial Homeostasis via the AMPK Signaling Pathway in Primary Cultured Neurons. *Environmental Pollution Elsevier Ltd.* <https://doi.org/10.1016/j.envpol.2020.114207>.
- Kuhlenbaumer, G., Berg, D., 2019. Parkinson disease genetics: too early to predict progression? *Nat. Rev. Neurol.* 15, 625–626. <https://doi.org/10.1038/s41582-019-0264-3>.
- Li, H., Hong, T., Zhu, Q., Wang, S., Huang, T., Li, X., Lian, Q., Ge, R.S., 2019. Paraquat exposure delays late-stage Leydig cell differentiation in rats during puberty. *Environ. Pollut.* 255, 113316. <https://doi.org/10.1016/j.envpol.2019.113316>.
- Li, H., Wu, S., Wang, Z., Lin, W., Zhang, C., Huang, B., 2012. Neuroprotective effects of tert-butylhydroquinone on paraquat-induced dopaminergic cell degeneration in C57BL/6 mice and in PC12 cells. *Arch. Toxicol.* 86, 1729–1740. <https://doi.org/10.1007/s00204-012-0935-y>.
- Li, H.Y., Wu, S.Y., Shi, N., 2007. Transcription factor Nrf2 activation by deltamethrin in PC12 cells: involvement of ROS. *Toxicol. Lett.* 171, 87–98. <https://doi.org/10.1016/j.toxlet.2007.04.007>.
- Liu, K., Zhan, Z., Gao, W., Feng, J., Xie, X., 2020. Cyclosporine attenuates Paraquat-induced mitophagy and pulmonary fibrosis. *Immunopharmacol. Immunotoxicol.* 42, 138–146. <https://doi.org/10.1080/08923973.2020.1729176>.
- Marras, C., Canning, C.G., Goldman, S.M., 2019. Environment, lifestyle, and Parkinson's disease: implications for prevention in the next decade. *Mov. Disord.* 34, 801–811. <https://doi.org/10.1002/mds.27720>.
- Martinez, J.H., Alaimo, A., Gorjod, R.M., Porte Alcon, S., Fuentes, F., Coluccio Leskow, F., Kotler, M.L., 2018. Drp-1 dependent mitochondrial fragmentation and protective autophagy in dopaminergic SH-SY5Y cells overexpressing alpha-synuclein. *Mol. Cell. Neurosci.* 88, 107–117. <https://doi.org/10.1016/j.mcn.2018.01.004>.
- Mostafalou, S., Abdollahi, M., 2017. Pesticides: an update of human exposure and toxicity. *Arch. Toxicol.* 91, 549–599. <https://doi.org/10.1007/s00204-016-1849-x>.
- Musgrove, R.E., Helwig, M., Bae, E.-J., Aboutalebi, H., Lee, S.-J., Ulusoy, A., Di Monte, D.A., 2019. Oxidative stress in vagal neurons promotes parkinsonian pathology and intercellular α -synuclein transfer. *J. Clin. Invest.* 129, 3738–3753. <https://doi.org/10.1172/JCI127330>.
- Nguyen, T.N., Padman, B.S., Lazarou, M., 2016. Deciphering the molecular signals of PINK1/parkin mitophagy. *Trends Cell Biol.* 26, 733–744. <https://doi.org/10.1016/j.tcb.2016.05.008>.
- Niu, K., Fang, H., Chen, Z., Zhu, Y., Tan, Q., Wei, D., Li, Y., Balajee, A.S., Zhao, Y., 2020. USP33 deubiquitinates PRKN/parkin and antagonizes its role in mitophagy. *Autophagy* 16, 724–734. <https://doi.org/10.1080/15548627.2019.1656957>.
- Ordenez, D.G., Lee, M.K., Feany, M.B., 2018. α -Synuclein induces mitochondrial dysfunction through spectrin and the actin cytoskeleton. *Neuron* 97, 108–124. <https://doi.org/10.1016/j.neuron.2017.11.036>.
- Pellacani, C., Costa, L.G., 2018. Role of autophagy in environmental neurotoxicity. *Environ. Pollut.* 235, 791–805. <https://doi.org/10.1016/j.envpol.2017.12.102>.
- Pringsheim, T., Jette, N., Frolkis, A., Steeves, T.D.L., 2014. The prevalence of Parkinson's disease: a systematic review and meta-analysis. *Mov. Disord.* 29, 1583–1590. <https://doi.org/10.1002/mds.25945>.
- Ramirez-Moreno, M.J., Duarte-Jurado, A.P., Gopar-Cuevas, Y., Gonzalez-Alcocer, A., Loera-Arias, M.J., Saucedo-Cardenas, O., Montes de Oca-Luna, R., Rodriguez-Rocha, H., Garcia-Garcia, A., 2019. Autophagy stimulation decreases dopaminergic neuronal death mediated by oxidative stress. *Mol. Neurobiol.* 56, 8136–8156. <https://doi.org/10.1007/s12035-019-01654-1>.
- Rani, L., Mondal, A.C., 2020. Emerging concepts of mitochondrial dysfunction in Parkinson's disease progression: pathogenic and therapeutic implications. *Mitochondrion* 50, 25–34. <https://doi.org/10.1016/j.mito.2019.09.010>.
- Rashidipour, M., Maleki, A., Kordi, S., Birjandi, M., Pajouhi, N., Mohammadi, E., Heydari, R., Rezaee, R., Rasouljan, B., Davari, B., 2019. Pectin/chitosan/tripolyphosphate nanoparticles: efficient carriers for reducing soil sorption, cytotoxicity, and mutagenicity of paraquat and enhancing its herbicide activity. *J. Agric. Food Chem.* 67 <https://doi.org/10.1021/acs.jafc.9b01106>.
- Reddy, P.H., Oliver, D.M., 2019. Amyloid beta and phosphorylated tau-induced defective autophagy and mitophagy in Alzheimer's disease. *Cells* 8, 488. <https://doi.org/10.3390/cells8050488>.
- Sartori, F., Vidrio, E., 2018. Environmental fate and ecotoxicology of paraquat: a California perspective. *Toxicol. Environ. Chem.* 100, 479–517. <https://doi.org/10.1080/0277248.2018.1460369>.
- Sathiyaseelan, P., Rothe, K., Yang, K.C., Xu, J., Chow, N.S., Bortnik, S., Choutka, C., Ho, C., Jiang, X., Gorski, S.M., 2019. Diverse mechanisms of autophagy dysregulation and their therapeutic implications: does the shoe fit? *Autophagy* 15, 368–371. <https://doi.org/10.1080/15548627.2018.1059609>.
- Song, M., Mihara, K., Chen, Y., Scorrano, L., Dorn, G.W., 2015. Mitochondrial fission and fusion factors reciprocally orchestrate mitophagic culling in mouse hearts and cultured fibroblasts. *Cell Metabol.* 21, 273–286. <https://doi.org/10.1016/j.cmet.2014.12.011>.
- Soutar, M.P.M., Kempthorne, L., Annuario, E., Luft, C., Wray, S., Ketteler, R., Ludtmann, M.H.R., Plun-Favreau, H., 2019. FBS/BSA media concentration determines CCCP's ability to depolarize mitochondria and activate PINK1-PRKN mitophagy. *Autophagy* 15, 2002–2011. <https://doi.org/10.1080/15548627.2019.1603549>.
- Stavoe, A.K.H., Holzbaur, E.L.F., 2019. Autophagy in neurons. *Annu. Rev. Cell Dev.*

- Biol. 35, 477–500. <https://doi.org/10.1146/annurev-cellbio-100818-125242>.
- Stotland, A., Gottlieb, R.A., 2015. Mitochondrial quality control: easy come, easy go. *Biochim. Biophys. Acta Mol. Cell Res.* 1853, 2802–2811. <https://doi.org/10.1016/j.bbamcr.2014.12.041>.
- Sun, D.Z., Song, C.Q., Xu, Y.M., Wang, R., Liu, W., Liu, Z., Dong, X.S., 2018. Involvement of PINK1/Parkin-mediated mitophagy in paraquat-induced apoptosis in human lung epithelial-like A549 cells. *Toxicol. Vitro* 53, 148–159. <https://doi.org/10.1016/j.tiv.2018.08.009>.
- Tremblay, R.G., Sikorska, M., Sandhu, J.K., Lanthier, P., Ribocco-Lutkiewicz, M., Bani-Yaghoub, M., 2010. Differentiation of mouse Neuro 2A cells into dopamine neurons. *J. Neurosci. Methods* 186, 60–67. <https://doi.org/10.1016/j.jneumeth.2009.11.004>.
- Wang, L., Yang, H., Wang, Q., Zhang, Qiaohui, Wang, Z., Zhang, Qunwei, Wu, S., Li, H., 2018a. Paraquat and MPTP induce alteration in the expression profile of long noncoding RNAs in the substantia nigra of mice: role of the transcription factor Nrf2. *Toxicol. Lett.* 291, 11–28. <https://doi.org/10.1016/j.toxlet.2018.04.002>.
- Wang, M., Miller, R.A., 2012. Fibroblasts from long-lived mutant mice exhibit increased autophagy and lower TOR activity after nutrient deprivation or oxidative stress. *Aging Cell* 11, 668–674. <https://doi.org/10.1111/j.1474-9726.2012.00833.x>.
- Wang, Q., Ren, N., Cai, Z., Lin, Q., Wang, Z., Zhang, Q., Wu, S., Li, H., 2017. Paraquat and MPTP induce neurodegeneration and alteration in the expression profile of microRNAs: the role of transcription factor Nrf2. *npj Park. Dis.* 3 <https://doi.org/10.1038/s41531-017-0033-1>.
- Wang, Q., Zhan, Y., Ren, N., Wang, Z., Zhang, Q., Wu, S., Li, H., 2018b. Paraquat and MPTP alter microRNA expression profiles, and downregulated expression of miR-17-5p contributes to PQ-induced dopaminergic neurodegeneration. *J. Appl. Toxicol.* 38, 665–677. <https://doi.org/10.1002/jat.3571>.
- Xu, X., Cui, Z., Wang, Xinlei, Wang, Xixin, Zhang, S., 2018. Toxicological responses on cytochrome P450 and metabolic transferases in liver of goldfish (*Carassius auratus*) exposed to lead and paraquat. *Ecotoxicol. Environ. Saf.* 151, 161–169. <https://doi.org/10.1016/j.ecoenv.2017.12.062>.
- Yamashita, S.I., Jin, X., Furukawa, K., Hamasaki, M., Nezu, A., Otera, H., Saigusa, T., Yoshimori, T., Sakai, Y., Mihara, K., Kanki, T., 2016. Mitochondrial division occurs concurrently with autophagosome formation but independently of Drp1 during mitophagy. *J. Cell Biol.* 215, 649–665. <https://doi.org/10.1083/jcb.201605093>.
- Yang, H., Lin, Q., Chen, N., Luo, Z., Zheng, C., Li, J., Zheng, F., Guo, Z., Cai, P., Wu, S., Wang, Y.-L., Li, H., 2020. LncRNA NR_030777 alleviates paraquat-induced neurotoxicity by regulating Zfp326 and Cpne5. *Toxicol. Sci.* 178, 173–188. <https://doi.org/10.1093/toxsci/kfaa121>.
- Zhang, Q., Hu, C., Huang, J., Liu, W., Lai, W., Leng, F., Tang, Q., Liu, Y., Wang, Q., Zhou, M., Sheng, F., Li, G., Zhang, R., 2019. ROCK1 induces dopaminergic nerve cell apoptosis via the activation of Drp1-mediated aberrant mitochondrial fission in Parkinson's disease. *Exp. Mol. Med.* 51 <https://doi.org/10.1038/s12276-019-0318-z>.
- Zhang, Z., Liu, L., Jiang, X., Zhai, S., Xing, D., 2016. The essential role of Drp1 and its regulation by S-nitrosylation of parkin in dopaminergic neurodegeneration: implications for Parkinson's disease. *Antioxidants Redox Signal.* 25, 609–622. <https://doi.org/10.1089/ars.2016.6634>.
- Zhao, G., Cao, K., Xu, C., Sun, A., Lu, W., Zheng, Y., Li, H., Hong, G.L., Wu, B., Qiu, Q.M., Lu, Z., 2017. Crosstalk between mitochondrial fission and oxidative stress in paraquat-induced apoptosis in mouse alveolar type II cells. *Int. J. Biol. Sci.* 13, 888–900. <https://doi.org/10.7150/ijbs.18468>.
- Zheng, F., Gonçalves, F.M., Abiko, Y., Li, H., Kumagai, Y., Aschner, M., 2020. Redox toxicology of environmental chemicals causing oxidative stress. *Redox Biol.* 101475. <https://doi.org/10.1016/j.redox.2020.101475>.